LNGS/EXP-01/06
April 2006

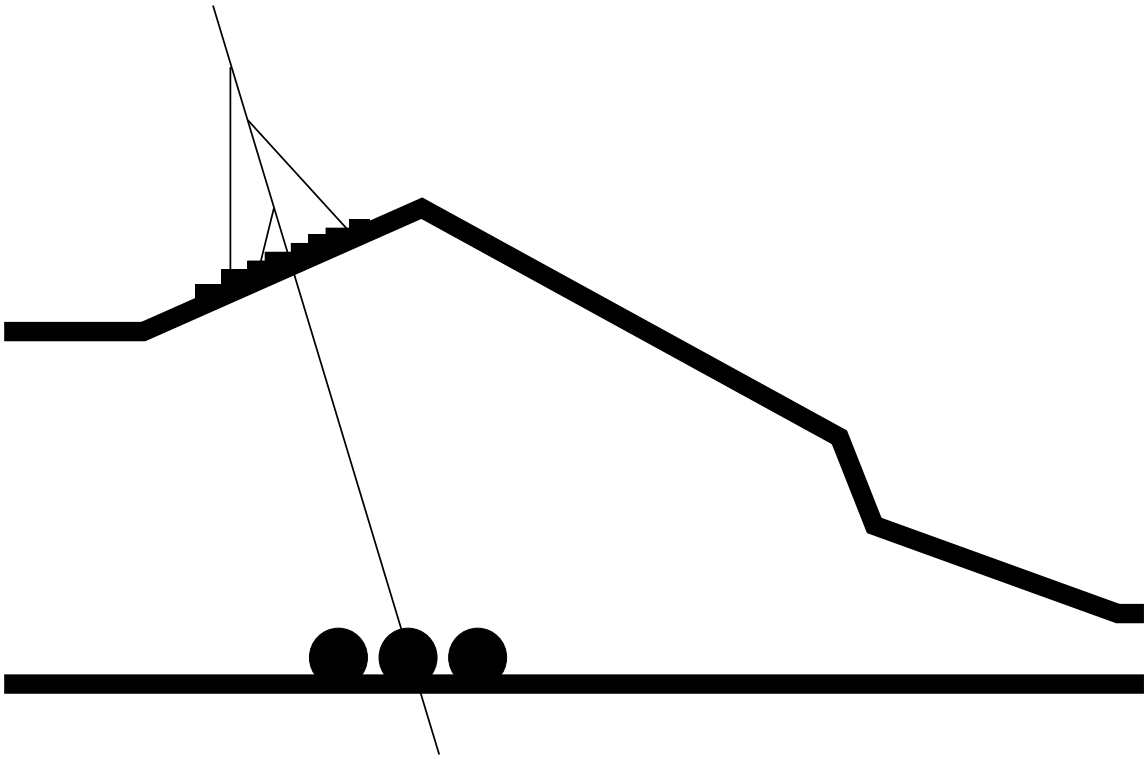

Purity measurements in Liquid Xenon. Electron lifetime dependence on circulation time and rate.

A.Ferella [a,b],
F. Arneodo [a], N. Canci[a,b], A. Corsi[a], B. Romualdi[a], A. Rotilio[a], E.Tatananni[a]

INFN - Laboratori Nazionali del Gran Sasso

INFN - Istituto Nazionale di Fisica Nucleare
Laboratori Nazionali del Gran Sasso

LNGS/EXP-01/06
April 2006

Purity measurements in Liquid Xenon. Electron lifetime dependence on circulation time and rate.

A.Ferella [a,b],
F. Arneodo [a], N. Canci[a,b], A. Corsi[a], B. Romualdi[a], A. Rotilio[a], E.Tatananni[a]

[a] *LNGS INFN - Italy*
[b] *Dipartimento di Fisica dell' Università de L'Aquila, Italy*

Abstract

Making profit of the experience acquired at LNGS in the purification of noble liquids, and in view of the installation of the XENON Dark Matter experiment, we started to collaborate wih the Columbia University about the measurement of the electron lifetime in Liquid Xenon (LXe). A dedicated setup, a small vessel containing a *Purity Monitor*, was built along with its cryogenic system. The setup was tested at LNGS and then at the Astrophysics Laboratories of Columbia University, where our vessel was inserted in an existing LXe purification chain. Two relatively long runs (from Feb. 23rd to Feb. 25th and from June 8th to June 15th) were carried out, during which the stability and the efficiency of the cryostat (a copper Cold Finger, insulated through fiber glass), the performances of a CsI photocathode (used as electron source) and, above all, the features of the Purity Monitor were tested. Before filling with Xenon, a particular procedure to clean the chamber and measure the contamination content in vacuum through an RGA was followed. The cooling rate of the Cold Finger was also measured. Finally the behavior of electron lifetime in Liquid Xenon versus recirculation time is shown; also the electric drift field dependence of τ_e is investigated, for fields ranging from 100 V/cm to 900 V/cm: these results suggest a contamination of CO_2 and N_2O, according to published data [14] and [15].

1 Introduction

The use of liquefied noble gases in ionization and scintillation Time Projection Chambers (TPCs) has been extensively investigated for various applications, ranging from gamma-ray astronomy [1], double beta decay [2][3][4], neutrino physics and proton decay [6][5], high energy physics at future hadron colliders [7] and recently dark matter search [8][9][10][11].

A fundamental requirement for any TPC based on liquefied noble gases is that the electrons produced by ionizing particles should travel undisturbed in the liquid from the point of production to the detection device. To this extent, the presence of any electro-negative impurity diluted in the liquid must be reduced to extraordinary low levels. Moreover the purity must be preserved at all time during the detector operation in order to ensure stable performance. This requirement is very strong in the case of the XENON Experiment, since it will look for rare events at extremely low energies.

A double phase Liquid Xenon Time Projection Chamber (LXeTPC) is under installation at LNGS for the XENON experiment, dedicated to the investigation of direct WIMP detection. The details of the detector are described elsewhere [9]. Here we briefly recall that the experiment exploits the scintillation emitted in LXe by ionization events ("primary scintillation"). Ionization electrons are then drifted by a strong (1 KV/cm) electric field towards the liquid surface where a stronger field extracts them causing proportional multiplication on a thin metallic grid. This last process gives origin to a second scintillation signal in gas (secondary scintillation). Both the primary and the secondary scintillation light are exploited in order to discriminate nuclear recoil (possibly induced by WIMP scattering) from other ionization events. The first phase foresees the installation of a 10 kg LXeTPC (XENON10) at the Gran Sasso Underground Laboratory. This detector has a maximum drift distance of the order of 20 cm, which requires an attenuation length of drifting electrons longer than one meter, or, equivalently, a value for the electron lifetime τ_e of the order of 1 ms. A dedicated system to study the feasibility of achieving such high purities in relatively big volumes (i.e. comparable to the XENON10 detector) has been built. The present note reports the results obtained in such a test. Its content is organized as follows: in section 2 is outlined the theory of the process of electron attachment on impurities; in section 3 we present a brief review of the Purity Monitor, the device used to measure the electron lifetime τ_e in Liquid Xenon and a detailed description of all its parts; section 4 describes the purification system; in section 5 are presented the performances of the cryostat used to maintain the chamber at Liquid Xenon temperature; then we show the measurements and discuss the data in section 6; finally in section 7 we present the conclusions and the proposal for some future activity.

2 Noble Liquids Purity and Electron Lifetime

.

The electron attachment to a generic electro-negative molecule of type S, diluted in the liquid, is characterized by two parameters: the attachment rate K_S and the concentration

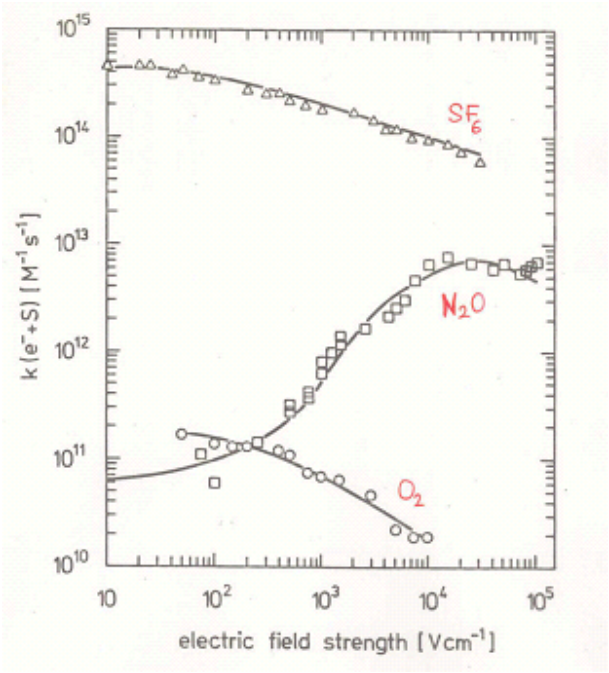

Figure 1: Dependence of the attachment rates by the electric field strength in Liquid Xenon for different kind of impurities [14]

of the impurities ρ_S. If a number $N_e(0)$ of electrons is produced in Liquid Xenon at time t=0, we would expect to find a reduced number of electrons at time t, according to the relation:

$$N_e(t) = N_e(0)\mathrm{e}^{-t/\tau_e} \tag{1}$$

where τ_e is the so called "*electron lifetime*", related to the impurity parameters by the relation:

$$\tau_e = \frac{1}{N_S K_S} \tag{2}$$

N_S is the number of the impurities. The rate K_S is a function of the electric field, as shown in figure 1. However, all the measurements that will be done in the XENON experiment by the Purity Monitor will be carried out in the range from 0.9 to 1.1 kV/cm, where the values of K_S can be considered almost constant to a good approximation.

Commercial Xe has a ppm concentration of many impurities (O_2, CO, N_2O, H_2O, plus several organic molecules) which absorb both drifting electrons and UV light. Unfortunately the xenon has a high affinity for polar molecules and thus is difficult to reach very low pollution levels. The XENON requirement is to reduce the concentration of electro-negative compounds to less then 1 ppb O_2 equivalent so to ensure the detection of

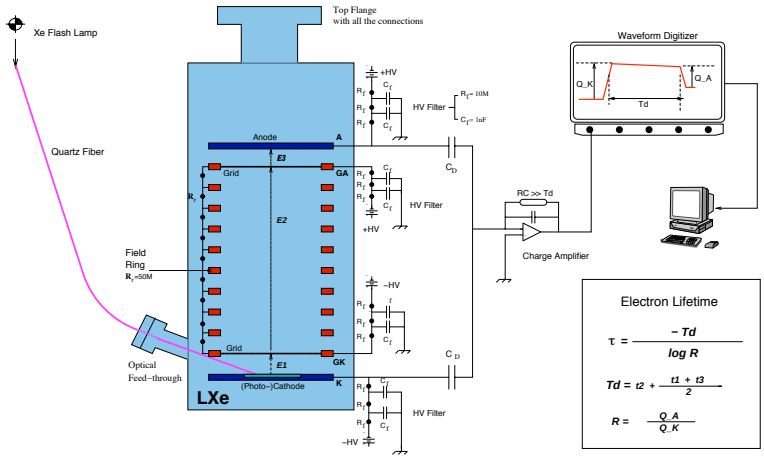

Figure 2: Layout of the PrM unit and read-out scheme

a signal of less then 20 electrons traveling for 30 cm drift gap. This is the charge produced by a 16 KeV nuclear recoil.

The LXe purity level must be monitored in the various phases of the detector operation (filling and running). A device, already developed and used by the ICARUS collaboration for the liquid Argon technology, the so-called *Purity Monitor* (PrM), and currently used by several experiments dealing with liquefied noble gases (ATLAS, EXO etc.), has been chosen to perform this job.

3 The Purity Monitor

To measure the purity level of Liquid Xenon, a dedicated Purity Monitoring System (PrM) has been designed and constructed at the Gran Sasso National Laboratory. It has been tested, during the month of February 2005 and, subsequently, in June 2005 in the Astrophysics Laboratory of Columbia University. The system has the same working principles of the one used by the ICARUS collaboration [12], but shows some differences in the materials used and for the adopted mechanical solutions. As shown in figure 2, the Purity Monitor consists of a small double-gridded drift chamber immersed in the LXe. Bunches of electrons are produced via photo-electric effect, flashing a photo-cathode with the UV light from a Xenon flash lamp guided on the photo-cathode by a quartz optical fiber. The electron cloud moves toward the anode along the electric field lines, crossing a drift region between two transparent parallel grids. The drifting photoelectrons induce a signal on the cathode. After having traveled through the drift region, some of them will reach the anode, inducing a current on it. Comparing the cathode and anode signals, we are able to estimate the concentration of impurities inside the liquid: if we suppose that the number of free electrons is much higher then the number of electro-negative molecules, the amount of missing electrons is proportional to the quantity of the impurities diluted in the liquid.

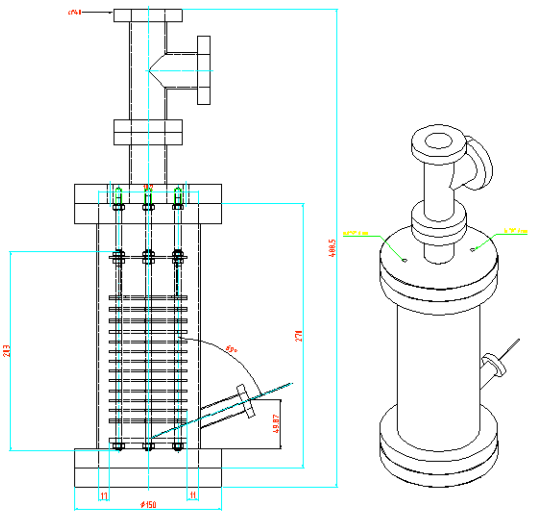

Figure 3: Drawing of the Purity Monitor Chamber.

The PrM is housed in a stainless steel vessel. On the top are the electrical feed-through, an analog and a digital high pressure gauges and a low pressure magnetic gauge. A turbo pump is directly connected to the chamber through a valve. Standard high vacuum techniques are used to assemble the chamber and connect it to the gas filling and vacuum system (see figure 2).

The drawing of the chamber is shown in figure 3.

3.1 The Structure

In figure 4 is sketched the geometry of the PrM. Its main structure is realized with stainless steel and Vespel, a high performance polyimide material (electrically insulating), formed from resin and with an excellent temperature resistance. Referring to figure 4, on the bottom there is the cathode disk where the photo-cathode is mounted (a CsI layer, 1 μm thick, deposited on a stainless steel disk, 2" diameter); the next electrode is the cathode grid (GK) placed at 10 mm from the cathode; a second grid (anode grid (GA)) facing the anode (a stainless steel plate). Between GA and GK there is a field-shaping system for the drift volume formed by an array of 9 rings, electrically connected by a resistor chain of 10 resistors, 30 $M\Omega$ each. The skeleton that supports the system is made with three Vespel rods and spacers to hold the electrodes and rings at fixed distances.

3.2 Photo-cathode and electrons extraction

It is the source of electrons to be necessary for the electron lifetime measurement. The precision on the lifetime determination depends on the actual signal-to-noise conditions

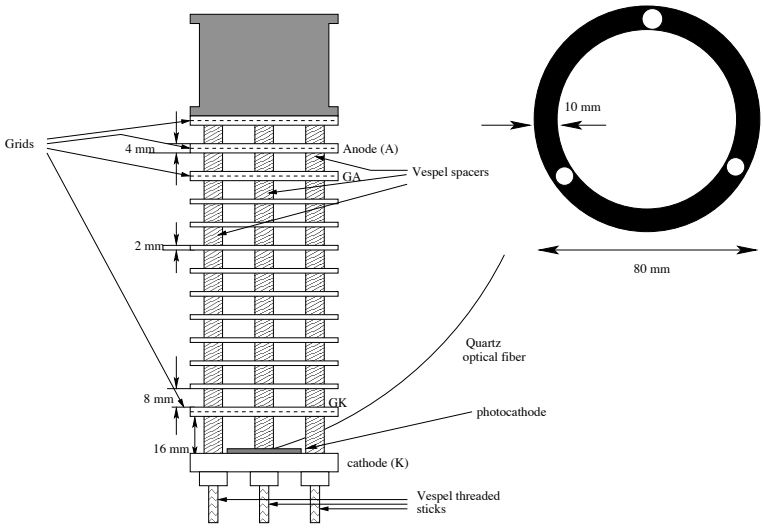

Figure 4: Purity Monitor geometry

provided by the system, the signal being the charge amplitude extracted from the cathode and subsequently collected by the anode. The optimal photocathode should therefore have the highest possible quantum yield and should be as well chemically very stable. A CsI layer deposited on metal substrate has proven to be, sofar, the best option. A quartz optical fibre ($\sim$1 mm core diameter, all silica) allows to guide the light (down to 180 nm of wavelength) from the source (a Xenon flash lamp placed outside the vessel) onto the photo-cathode. A dedicated feed-through (Fig. 5) for the fiber is directly connected through a standard ConFlat flange to the Purity Monitor chamber and the fiber is held by a hollowed vespel rod that keeps the fiber end at a distance of 2 mm from the cathode centre and at an angle of 20^o to the cathode plane. The light source is a ORIEL 63501 illuminator system, equipped with a ORIEL 6427 Xenon bulb. This system focalizes the light onto the fiber tip by means a spherical mirror. The FWHM of the pulse is 9 μs and the arc size is 3 mm.

3.3 Electron drift fields

We used four independent High Voltage channels to drive the electrodes (K, GK, GA, A). In the drift zone (i.e between the two grids) the maximum electric field value used was 900 V/cm, close to the operational field of the XENON experiment, that is 1000 V/cm.

3.4 Signal readout electronics

A system has been designed for the read-out and storing of the charge information from the PrM unit. It is composed by (1) a Decoupling Stage formed by a HV filter and a capacitor (C_D), (2) a single Charge Sensitive Amplifier and (3) a Waveform Digitizer,

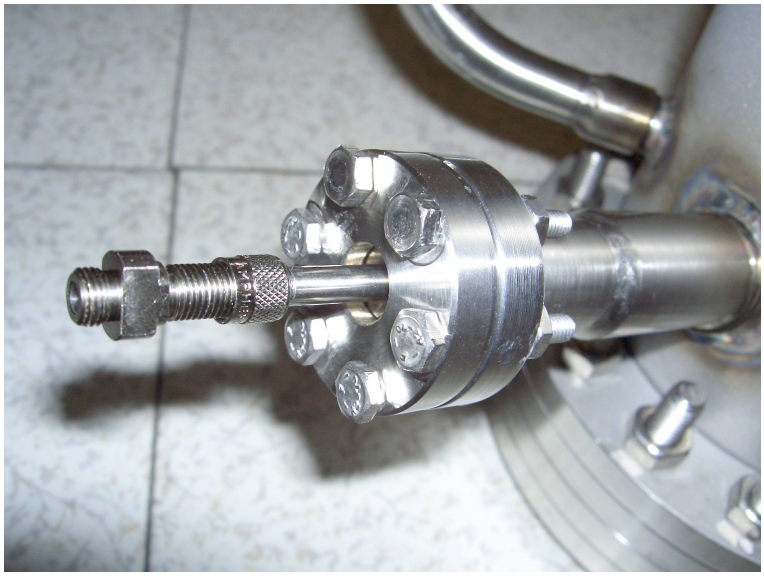

Figure 5: The fiber optics feed trough

see Fig. 2. A cylindrical aluminium case, mounted directly on the electrical feed-through (outer side), hosts the Decoupling Stage as well as the Amplifier (AMPTEK - A250) (Fig. 6). On the top flange of the case there are the HV input and output signal connectors. This setup minimizes ambient noise pick-up and the amplifier input capacitance due to the signal cable length. Both anode and cathode signals feed the input stage of the same amplifier (AC coupling), so to avoid the necessity of an cross-calibration of two analog gains. The current signals from the anode and the cathode are opposite in sign. Therefore, the charge amplifier output signal results in a trapezoidal waveform, whose three main features (falling edge, flat bottom, rising edge) correspond to the three drift gaps of the Purity Monitor (Fig. 15).

4 The Purification process

A schematic drawing of the purification and gas handling system is shown in Fig. 7. The commercial Xenon Gas was initially stored in a 3,8 l stainless steel cylinder. The purification system, along with the gas filling and recuperation lines, was built with 1/4" pipes and standard VCR 1/4" connections, welded or made with high vacuum fittings, all stainless steel. The valves used were all-metal, bakeable ones. Before running the experiment the entire system was evacuated with a turbo molecular pump. Furthermore the gas line was baked at more than 200 ^{o}C.

We also performed several baking cycles on the chamber at lower temperature (about 120 ^{o}C), to avoid damage to the optical fiber sheath. At the end of each cycle we analyzed the residual gases in the chamber via an RGA. When an acceptable level of residual gases

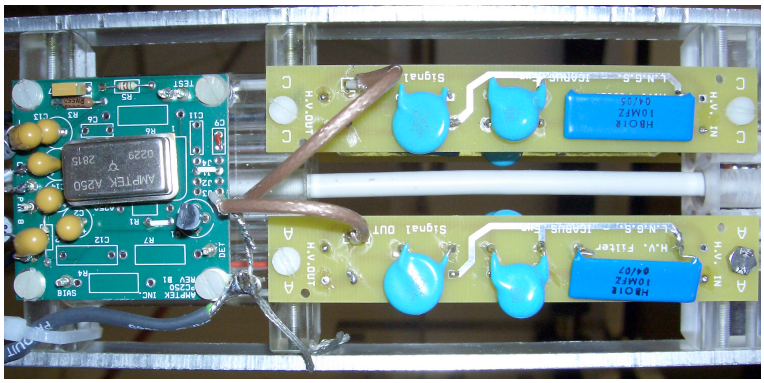

Figure 6: Picture of the Front-end electronics

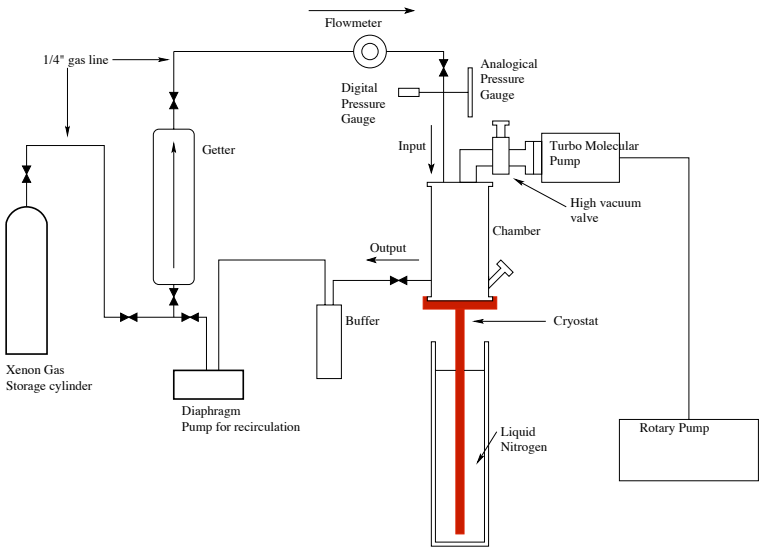

Figure 7: Schematic of the Liquid Xenon purification system

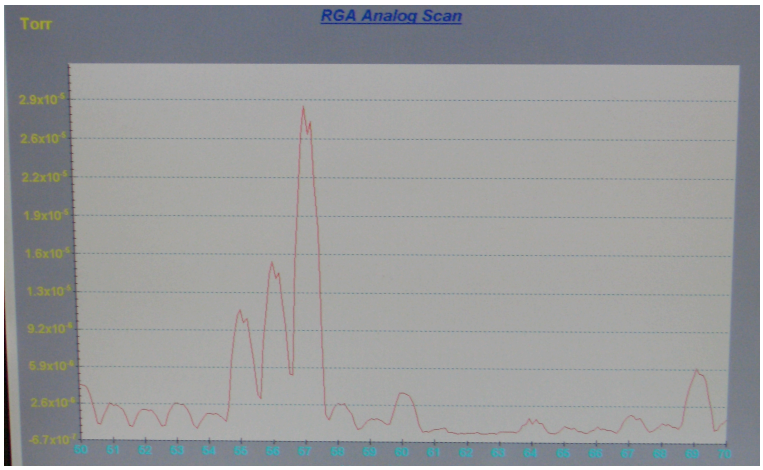

Figure 8: RGA spectrum

was reached, the vessel was finally flushed with Xenon gas. In Fig. 8 is presented one of the spectra we obtained after a cycle of more then 2 hours of baking. The final outgassing rate was $4 \cdot 10^{-7}$ $mbar\ l/s$.

It has to be noticed that in the first test the chamber had been kept under vacuum for a few days whereas the second run was carried out after more than two months of pumping. Moreover, during the period of time between the two tests it has been also baked several times. As we will see, the result of this long baking time was that the chamber did not present an appreciable impurities content.

Once the system was clean, we filled the chamber with Xenon gas purified through a MonoTorr Phase II heated getter, made by Saes Getter. Using a cryostat based on the heat transfer between the chamber and a Liquid Nitrogen bath (the main features of this system are presented in section 5), the Purity Monitor vessel was cooled down in order to liquefy the Xenon gas we were flowing into it. With a gas flow rate of about 2.3 l/m, it took approximately 2.5 hours to fill the chamber. When Liquid Xenon had reached the anode, we closed the valve of the storage cylinder and started the recirculation, with a diaphragm pump. The system was stable with a flow rate of 2.8 l/m. In this way the time that the entire volume of liquid contained in the chamber takes to pass (in gas phase) through the getter can be calculated and thus we can estimate how many cycles are needed to reach a prefixed purity.

5 Cooling System

One of the difficulties of dealing with the LXe is the cost. One liter of LXe costs a thousand dollars or more. This makes it impossible to use an external, open LXe bath to cool the vessel of the PrM, as it can be done with Liquid Argon. Different solutions are possible, such as the use of mixtures of Liquid Nitrogen and alcohol, or pressurized

Nitrogen etc. An interesting, cost effective and (theoretically simple) solution is the *cold finger* technique, which consists in putting the vessel in thermal contact with a copper rod, whose other end is immersed in a Liquid Nitrogen bath. This solution is very attractive but it is not trivial to calculate a priori the exact dimensions of the rod.
We recall that at atmospheric pressure Xe stays liquid between 153 and 163 K. In this section we present the design of the cold finger, built according to the calculations made on the heat transfer through a 100 cm long copper rod partially immersed (30 cm) in a bath of Liquid Nitrogen and in thermal contact on its top with the PrM chamber. Covering the PrM chamber by a styrofoam tube that provides the thermal insulation of the system, and considering a flow rate of about 5 liter of xenon gas per minute (a loss of about 50 W due to the liquefaction of such amount of gas), we are able to determine what radius the copper rod should have in order to maintain the system in thermal equilibrium at Liquid Xenon temperature (see next section and Fig. 10 for further details).

5.1 Design, drawings and construction of the cryostat

The heat transfer (ΔQ) in a time Δt from a body at temperature T_1 to a body at temperature T_2 (with $T_1 > T_2$) through a rod of material with cross-sectional area A and length L is given by the simple formula:

$$\frac{\Delta Q}{\Delta t} = kA\frac{T_1 - T_2}{L} \tag{3}$$

where k is the *thermal conductivity* of the rod.

The values of the k constant for copper and styrofoam are, respectively, $k_{Cu} = 385J \cdot s^{-1} \cdot m^{-1} \cdot (C^\circ)^{-1}$ and $k_{Sty} = 0.01j \cdot s^{-1} \cdot m^{-1} \cdot (C^\circ)^{-1}$

The external radius of the chamber is 6 cm, so the styrofoam tube surrounding it should have the internal radius of 6 cm and the external radius of 10 cm or more. From the equation 3 we find that the power lost by the tube, supposing the internal temperature $T_2 = -110C^\circ$ and the external environmental temperature $T_1 = 23C^\circ$, is 5.6 $Watt$.

We can use this datum to calculate the radius of the copper rod, supposing a total power loss, including also the recirculation (50 Watt). From the equation 3 we find that the cross-sectional area of the copper rod should be:

$$A = \frac{L \cdot P}{(T_1 - T_2) \cdot k} = 0.0016 \text{ m}^2 \tag{4}$$

to which corresponds a radius (r) of 2.25 cm.

According to the previous calculations we realized a copper rod 100 cm long and with a diameter of 5 cm. The cold finger ends with a squared cross section which allows the installation of 4 thermal resistors used to supply heat to the system, if necessary, in order to maintain the temperature desired. The top of the rod sustains a copper plate that is placed in thermal contact with the bottom of the Purity Monitor chamber. Furthermore we added a copper shield around the vessel in thermal contact with the upper plate of

the cold finger in order to improve the thermal conduction of the system and to allow a uniform temperature inside the chamber.

A scheme of the cryostat is shown in Fig. 10, while in Fig. 9 is a picture of the Cold Finger without any thermal insulation.

x

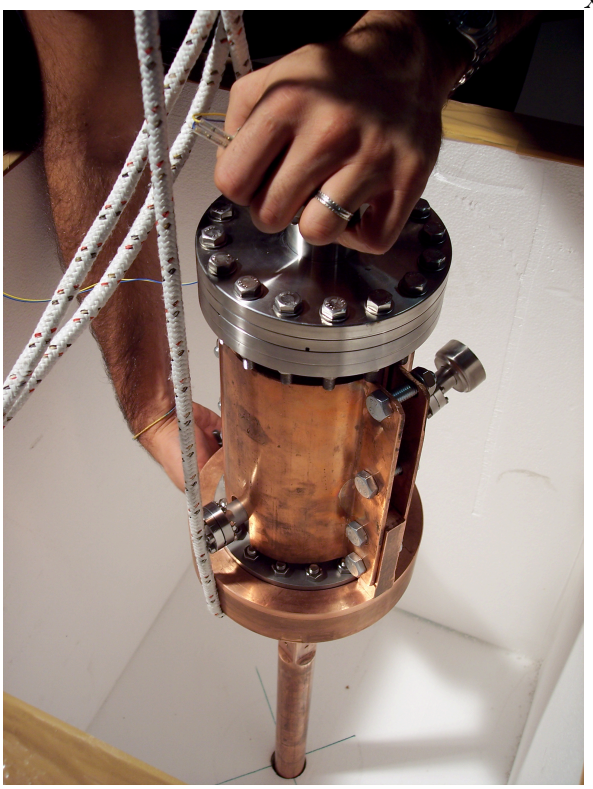

Figure 9: Picture of the cold finger, taken during our test at LNGS

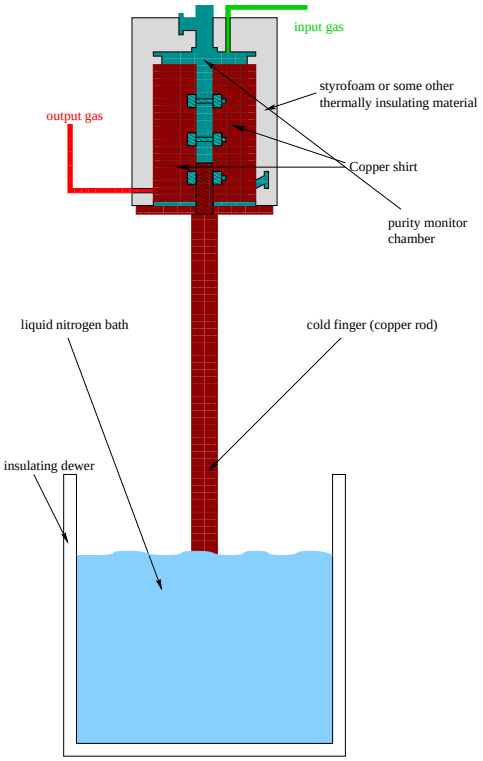

Figure 10: Sketch of the final configuration of the system; the cold finger, immersed in the Liquid Nitrogen bath, in its upper part is in thermal contact both with a copper plate hosting the bottom flange of the chamber and with a copper shield surrounding the chamber itself.

5.2 Performance of the cryostat and tests

The performances of the system have been demonstrated at the Gran Sasso Laboratory using gaseous argon and measuring the temperature of the gas inside the vessel. In these tests we reached and maintained the temperature of -110^{o}C for 30 minutes. To

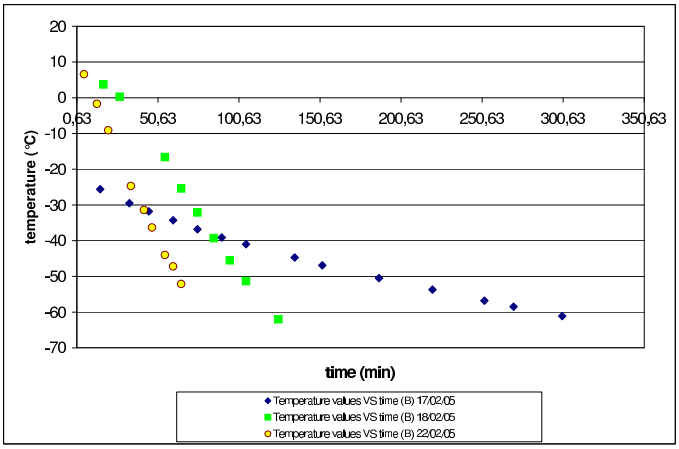

Figure 11: Temperature measurements inside the PrM chamber, during three different cooling tests

help temperature stabilization and to simulate the power loss due to the recirculation, electrical current was fed through the four resistors (25 W each) attached to the copper rod.

At the Astrophysics Laboratories of Columbia University those results had to be reproduced in Liquid Xenon. Because of the different set-up, the CF had been cut 30 cm off in order to have the right ratio between the immersed and the emerging parts. The chamber was filled with Liquid Xenon and the temperature and the system was maintained stable even when the recirculation was on.

In Figure 11 we report the comparison between the cooling rate of three different measurements: the green points are the values of the temperatures that we measured inside the chamber when we were trying to use the full length version of the Cold Finger, the other points (blue and yellow) are the values taken with the shorter copper rod. We can notice the different slope of the three curves, due to the higher cooling power of the improved (shortened) Cold Finger.

6 Electron Lifetime measurements

The high voltage was raised as soon as we filled the chamber with LXe. We used different sets of fields, from 100 V/cm to 900 V/cm, at steps of 100 V/cm. One of the waveforms recorded with the PrM in Liquid Xenon during the test is shown in Fig. 15. The measurement of the rise and fall amplitudes (corresponding to Q_K and Q_A), along with the pulse duration (the drift time T_d) gives a direct estimation of τ_e at the time of the measurement,

according to the equation:

$$\frac{Q_A}{Q_K} = \mathrm{e}^{-\frac{\Delta T}{\tau_e}} \tag{5}$$

Thus, calling R the ratio $\frac{Q_A}{Q_K}$, the electron lifetime is going to be equal to:

$$\tau_e = -\frac{\Delta t}{ln(R)} \tag{6}$$

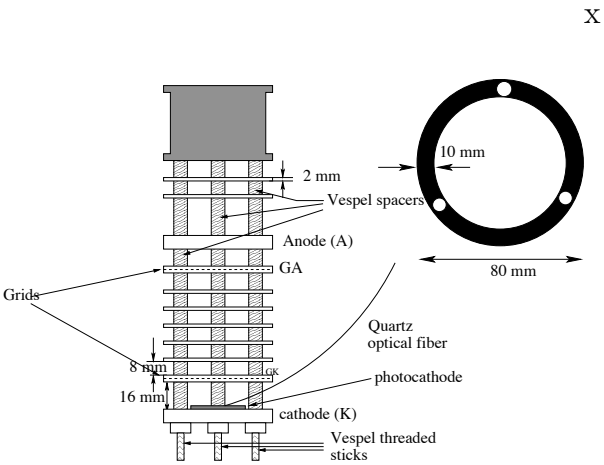

Figure 12: Geometry of the Purity Monitor used in these tests

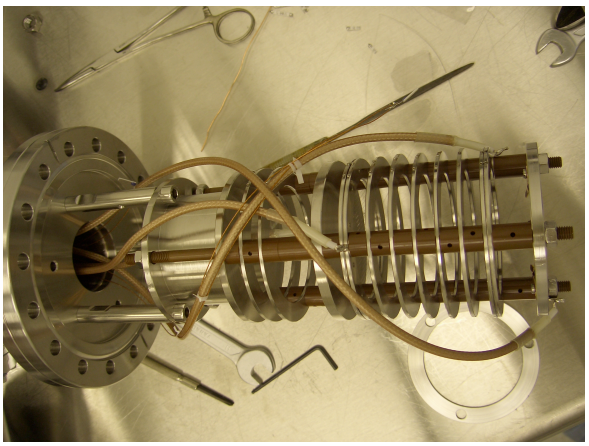

Figure 13: A picture of the Purity Monitor

It can be noticed that the ratio $R = \frac{Q_A}{Q_K}$ is strongly related to the Liquid Xenon purity. Fluctuations on the electron charge extracted and electronics noise, both affecting the signal amplitude, limit the precision on the determination of the lifetime, particularly for low τ_e values. The range of sensitivity (i.e. where τ_e is measured with a given precision) can be tuned according to the drift time (derived from the drift velocity, see Fig. 17) chosen by appropriate HV biasing of the electrodes.

6.1 Waveform fit function

We used an analytical fit to extract the required physical informations from the PrM waveforms. The parameters of the fit are the drift time and the anode and cathodic charges.

We performed two independent fits to determine these three parameters: a Fermi-Dirac function (time variable) is used both for cathodic and for anode signal amplitudes. The drift time is computed by subtracting the time when the anode amplitude is at half maximum from the time when the cathodic amplitude is at half maximum (we are

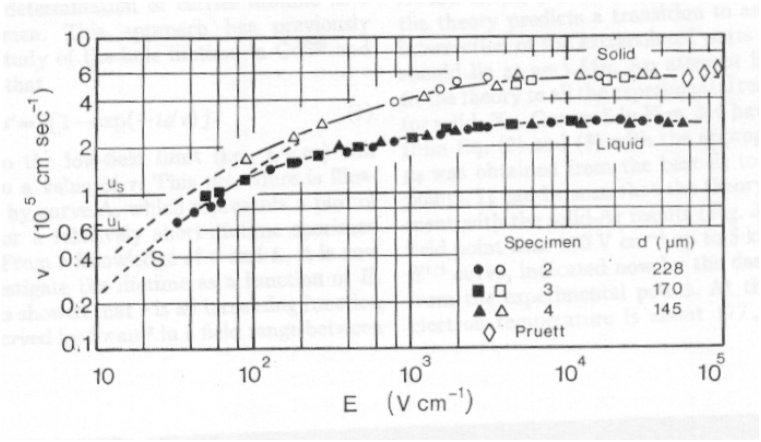

Figure 14: Drift velocity versus electric drift field [13].

referring to absolute values of the amplitudes of the signals, see Fig. 16). The expression of the cathodic fit is:

$$F_{cat} = p_0^c + \frac{p_1^c}{1 + \mathrm{e}^{\frac{t-p_2^c}{p_3^c}}} \tag{7}$$

The expression of the anode fit is:

$$F_{an} = p_0^a - \frac{p_1^a}{1 + \mathrm{e}^{\frac{t-p_2^a}{p_3^a}}} \tag{8}$$

where p_i are the fit parameters, from which we can deduce the cathodic and anode charge (Q_k and Q_a respectively) and the drift time (t_d):

$$Q_k = p_1^c \qquad Q_a = p_1^a \qquad t_d = p_2^a - p_2^c \tag{9}$$

6.2 Results

The first run lasted for more then two entire days, from Feb. 23rd to Feb. 25th. During this period the recirculation was on and the gas was continuously purified by the getter. In Figure 14 we report the time evolution of the lifetime and of the anode signal (in mV). It can be noticed that the electron lifetime significantly increased, from the beginning to the last measurements. It can be noticed too, that the τ_e curve has not a monotone behavior, but it oscillates especially at the beginning of the run. This fact is due to the instability of the flow rate, that at the beginning was very unstable. When the flow rate is too high the getter is not able to purify all the gas which passes through it and, since the detector is being cleaned by the gas itself, the gas gets dirtier. It can be also seen from the same plot that the electron lifetime, as it should be, changes with the anode charge,

x

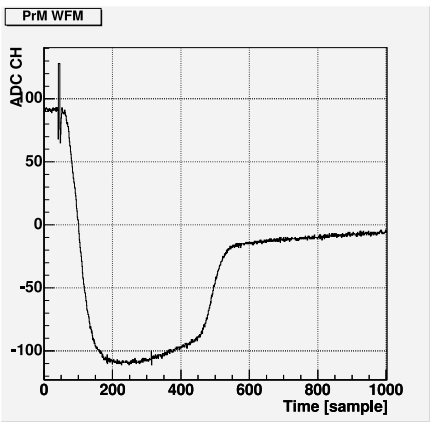

Figure 15: Purity Monitor waveform taken at 400 V/cm drift field

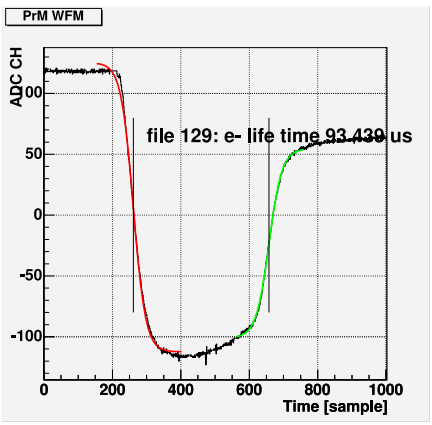

Figure 16: Purity Monitor waveform with fit taken at 400 V/cm drift field

while the cathode signal is almost constant (we operated always at the same field of 400 V/cm in the drift region and the power of the flash lamp was fixed). The red triangles are the values of the lifetime measured directly from the scope (i.e. taken by measuring from the trapezoidal waveform on the scope, the amplitude of anode and cathode signals and the time Δt and computing the lifetime by means of equation 6) the black points are the values coming from the fit . The maximum value of the electron lifetime we measured in this test was $110\mu s$ compared to an initial value of $18\mu s$.

The second test was longer than the first one and gave the most interesting results. The experiment ran continuously for more than seven days, from the 8th to the 15th June 2005 always at an electric drift field of 200 V/cm. During this period we tried to operate in three different conditions in order to investigate how the temperature influences the value of the lifetime: a) normal conditions of pressure (between 1.5 and 2.5 Atm), b) at very high pressure (more than 4 Atm), c) at very low pressure (less than 1 Atm). In figure 18 we report the evolution of the lifetime and of the drift time as a function of the recirculation time (plot on top and in the middle, respectively), and in the bottom plot the temperature variation during each measurement. As usual, the red points are the "hand made" measurements whereas the black points are the data coming from the fit.

During the fist entire day we kept the system at steady conditions in order to reach higher values of the electron lifetime. Then, as can be noticed by the figure, we increased the pressure, i.e. increased the temperature, and saw that the lifetime decreased, because the higher the temperature, the more impurities dilute in the liquid. After this phase, during the next day we tried to come back to higher values of the lifetime. We reached a value of 300 μs. We lowered the temperature in order to solidify the Liquid Xenon and see if the Monitor was still effective and estimate the electron drift velocity in Solid Xenon.

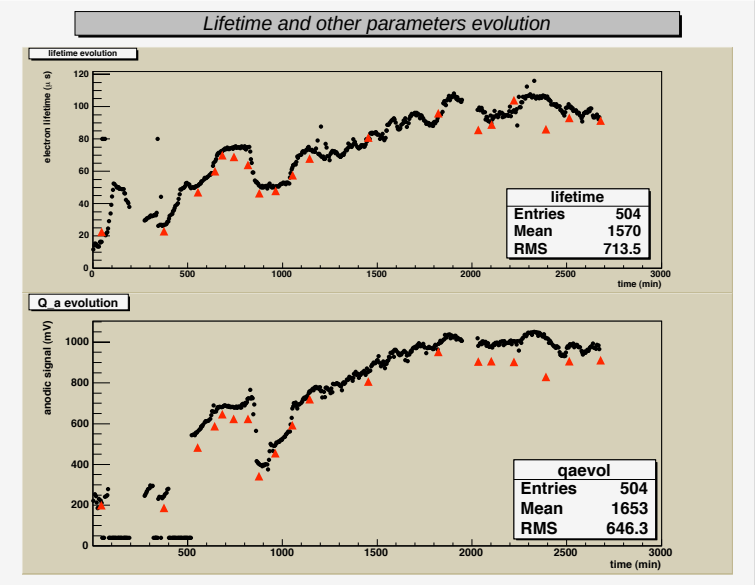

Figure 17: Time evolution of all the parameres.

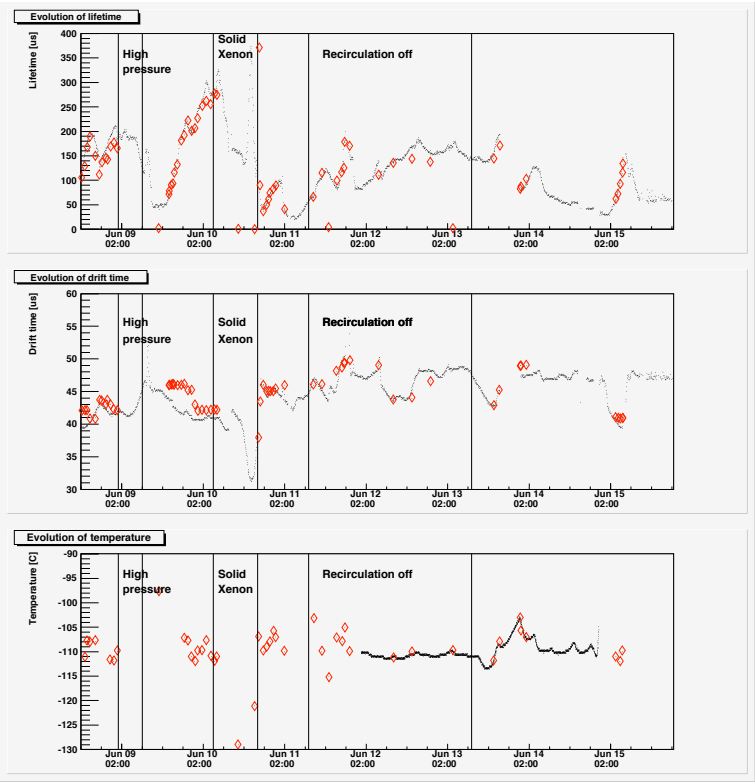

Figure 18: Time evolution of electron lifetime (top), drift time (middle) and temperature (bottom).

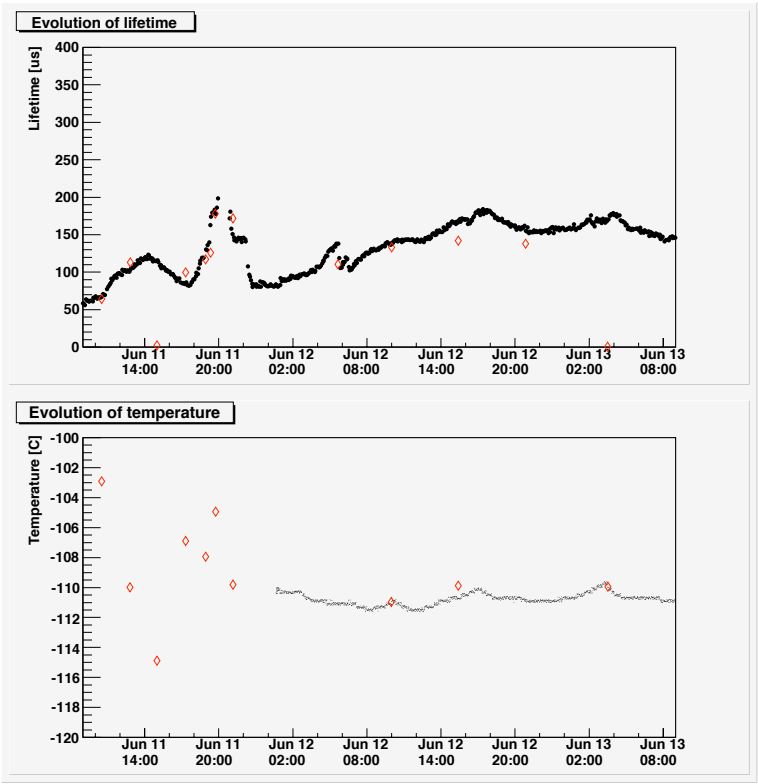

Figure 19: Time evolution of electron lifetime (top) and temperature (bottom) without recirculation. The red diamonds are the "hand-made" measurements.

It can be noticed that as soon as the liquid starts to solidify, the drift time decreases, as expected. When also the anode is completely covered by the solid, the electron lifetime is much higher than before, as shown in the figure (the peak at more than 350 μs).

We obtained the most important results of this test during the last few days, when we closed the recirculation and analyzed the behavior of the electron lifetime. In figure 19 are shown the lifetime and temperature evolution in the chamber. It has to be noticed that during this period the data were acquired automatically (both from the scope for the waveforms and from the digital temperature and pressure gauges). The top plot of the figure 19 shows that the lifetime remains almost constant during the whole period when the recirculation was off, that means that our Purity Monitor is not itself a source of impurities, and that cleaning and baking procedures were effective.

In Fig. 21 and 20 we report the electron lifetime versus the electric drift field during the February and June tests respectively. There is an evident dependence of the electron lifetime (τ_e) on the electric field strength (E), i.e., more precisely, the higher E the lower τ_e. We believe that this behavior, obviously stronger in the first test than in the second, is due to CO_2 and N_2O contamination inside the liquid, according to the data reported in Fig. 1. In a future test we expect to see a complete removal of these molecules.

x

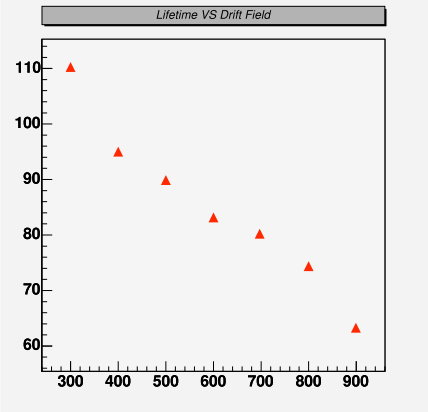

Figure 20: Electron lifetime as function of the electric drift field (February 2005)

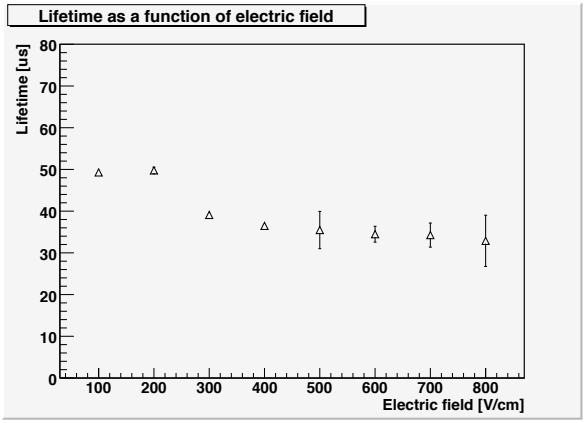

Figure 21: Electron lifetime as function of the electric drift field (June 2005)

7 Conclusions

A system for the measurement of the electron lifetime of noble liquids, originally designed for Argon, was successfully tested in Liquid Xenon. This Purity Monitor was built at the Gran Sasso Laboratory and then tested in LXe at the Nevis Laboratory of the Columbia University, in cooperation with the XENON Dark Matter Collaboration. A simple, cost effective system to cool down the vessel containing the PrM (Cod Finger) was designed and realized at the Gran Sasso Laboratory and worked in an excellent way. The system measured successfully electron lifetimes up to 300 μs. The electron lifetime of the liquid remained stable even in absence of recirculation, showing that the employed materials do not pollute the liquid.

The two future steps will be:

- use the PrM for a longer test aiming at longer lifetimes ($\geq 1\ ms$)
- design a new version of Purity Monitor (thinner than the one we used in the tests discussed in this report) to be installed inside the XENON10 and in the final XENON 1Ton detector.

8 Acknowledgements

This work was partly supported by a PRIN 2003 grant of Ministero dell'Istruzione, Università e Ricerca. We thank all the members of the XENON experiment for their warm collaboration and particularly the spokesperson, Prof. Elena Aprile, and Karl Giboni, Masaki Yamashita, Pawel Majewski.

References

[1] E. Aprile and M.Suzuki, IEEE Trans. Nucl. Sci. 36 (1989) 311 and XENON publications web page.
http://www.astro.columbia.edu/ lxe/XENON/2004/11/publications.html

[2] D.A.Imel and J.Thomas, Nucl. Inst. and Met. A273 (1988) 291

[3] A.S.Barabash et al., Preprint of Inst. of Exp. and Theor. Phys., Moscow, 1986, 154

[4] M.Danilov et al. (EXO Collaboration), Phys. Lett. B480 (2000) 12

[5] Y.Suzuki 2001, Proc. Int. Workshop on Low Energy Solar Neutrinos LowNu2 (Tokyo, Japan, 4-5 Dec. 2000) ed. Y.Suzuki (Singapore: World Scientific)

[6] ICARUS Initial Physics Program, ICARUS-TM/2001-03, LNGS P28/01, LNGS-EXP 13/89 add.1/01

[7] ATLAS Collaboration, CERN/LHCC/94-43, LHCC/P2, 15 December 1994

[8] R.Brunetti et al., proceeding for Dark Matter 2004, astro-ph/0405342, WARP proposal, http://warp.pv.infn.it/proposal.pdf

[9] XENON Collaboration, Nuclear Physics B (Proc. Suppl.) 138 (2005) 156159

[10] P. Belli et al., Il Nuovo Cimento A 103 (1990) 767

[11] W.G.Jones et al., Ed. N J C Spooner, (World Scientific), 428-433

[12] G.Carugno et al., Nucl. Inst. and Met. A292 (1990) 580-584

[13] L.S.Miller, S.Howe, W.E.Spear, Phys. Rev. 166 (1968), 871

[14] G.Bakale U.Sowada and W.F.Schmidt, J.Phys. Chem. 80 (1976) 2556

[15] S.D.Biller et al., Nucl. Inst. and Met. A276 (1989) 144